ISSN 1063-7710, Acoustical Physics, 2017, Vol. 63, No. 2, pp. 204–215. © Pleiades Publishing, Ltd., 2017.

ACOUSTICAL ECOLOGY. NOISE AND VIBRATION

Sonar Inter-Ping Noise Field Characterization During Cetacean Behavioral Response Studies off Southern California[1]

Shane Guan[a, c, *], Brandon L. Southall[b], Joseph F. Vignola[c], John A. Judge[c], and Diego Turo[c]

[a] *Office of Protected Resources, National Marine Fisheries Service Silver Spring, MD 20910*

[b] *SEA, Inc., Aptos, CA 95003, and University of California, Santa Cruz Santa Cruz, CA 95064*

[c] *Department of Mechanical Engineering, The Catholic University of America Washington, DC 20064*

**e-mail: shane.guan@noaa.gov*

Received January 15, 2016

Abstract—The potential negative effects of sound, particularly active sonar, on marine mammals has received considerable attention in the past decade. Numerous behavioral response studies are ongoing around the world to examine such direct exposures. However, detailed aspects of the acoustic field (beyond simply exposure level) in the vicinity of sonar operations both during real operations and experimental exposures have not been regularly measured. For instance, while exposures are typically repeated and intermittent, there is likely a gradual decay of the intense sonar ping due to reverberation that has not been well described. However, it is expected that the sound field between successive sonar pings would exceed natural ambient noise within the sonar frequency band if there were no sonar activity. Such elevated sound field between the pings may provide cues to nearby marine mammals on source distances, thus influencing potential behavioral response. Therefore, a good understanding of the noise field in these contexts is important to address marine mammal behavioral response to MFAS exposure. Here we investigate characteristics of the sound field during a behavioral response study off California using drifting acoustic recording buoys. Acoustic data were collected before, during, and after playbacks of simulated mid-frequency active sonar (MFAS). An incremental computational method was developed to quantify the inter-ping sound field during MFAS transmissions. Additionally, comparisons were made between inter-ping sound field and natural background in three distinctive frequency bands: low-frequency (<3 kHz), MFA-frequency (3–4.5 kHz), and high-frequency (>4.5 kHz) bands. Results indicate significantly elevated sound pressure levels (SPLs) in the inter-ping interval of the MFA-frequency band compared to natural background levels before and after playbacks. No difference was observed between inter-ping SPLs and natural background levels in the low- and high-frequency bands. In addition, the duration of elevated inter-ping sound field depends on the MFAS source distance. At a distance of 900–1300 m from the source, inter-ping sound field at the exposure frequency is observed to remain 5 dB above natural background levels for approximately 15 s, or 65%, of the entire inter-ping interval. However, at a distance of 2000 m, the 5 dB elevation of the inter-ping SPLs lasted for just 7 s, or 30% of the inter-ping interval. The prolonged elevation of sound field beyond the brief sonar ping at such large distances is most likely due to volume reverberation of the marine environment, although multipath propagation may also contribute to this.

Keywords: underwater noise, sonar, marine mammal, behavioral response, reverberation

DOI: 10.1134/S106377101702004X

INTRODUCTION

How military sonar may negatively affect marine mammals (primarily cetaceans which include whales and dolphins) has been a subject of significant research, conservation, and regulatory interest for the past several decades. Numerous cetacean mass stranding events resulting in mortality have been associated with naval exercises involving mid-frequency (1–10 kHz) active sonar (MFAS) operations [1–5]. Although a definitive mechanism of the mass stranding is unknown, some researchers have found gas emboli in stranded animals [6, 7]. Additional analyses based on acoustic propagation modeling and animal locations suggest that these outcomes may not result directly simply from high levels of sound exposure, but that the animals' behavioral response to the MFAS exposure may play a more indirect, but important mediating role in the stranding [4, 5, 8]. Different types and magnitudes of behavioral responses may be expected to occur depending on the interaction of received sound level and a variety of sound exposure conditions [9]. Consequently, considerable efforts are being devoted to reveal the potential behavioral responses of marine mammals to MFAS exposure [10]. Nevertheless, con-

[1] The article is published in the original.

sidering the more complex nature of contextual variables that appear to drive response probability beyond the simple received sound level considered in many earlier studies, more comprehensive quantification of sound exposure is clearly needed.

The acoustic field in the vicinity of sonar operations is likely to experience a gradual decay of the high sound pressure levels (SPLs) after the termination of the ping due to reverberation. Therefore, it is expected that the sound field between successive sonar pings (e.g., during the inter-ping interval) would exceed natural ambient noise within the sonar frequency band if there were no sonar activity. Such elevated sound field reverberation characteristics, and the information it may convey about proximity and/or relative orientation of source and receiver, thus has the potential to affect the probability of marine mammal behavioral responses to MFAS beyond the initial direct-path exposure. Where these frequencies overlap, they may also mask biological signals that are important to the life functions of marine mammals [11]. In order to provide a thorough assessment of behavioral response and acoustic masking potential in an environment influenced by MFAS, it is important to understand the reverberant field. However, among the large and growing number of studies being conducted on noise impacts to marine life over the past decades, few investigations have characterizing the reverberant field from anthropogenic noises [12, 13] or explicitly addressed concerns of reverberant field on marine mammal behavioral responses and acoustic masking [11]. Specifically, no research that the authors are aware of addresses the potential of acoustic masking from tonal sources, and only occasionally tonal masking is discussed in relation to noise impacts to marine mammals (e.g., Richardson et al. [14] and Au and Hastings [15]).

To address some of these information gaps and quantify relevant sound field characteristics resulting from intense anthropogenic transient tonal noises such as military sonar, we measured and analyzed the soundscape in the vicinity of a conducted during a subset of experimental sonar experiments involving controlled exposure experiments (CEEs) with simulated MFAS (described in Southall et al. [10]). The objectives of this study are to (1) use a quantitative method to analyze a simulated MFAS inter-ping sound field levels; (2) compare the inter-ping sound field among different frequency bands; (3) compare the inter-ping sound field between the time of simulated MFA playbacks and that of pre- and post-playbacks; (4) investigate the relationship between the inter-ping sound level and the distance of MFAS source; and (5) investigate the inter-ping sound field decay at different distances from the source.

MATERIALS AND METHODS

Passive Acoustic Data Collection

An interdisciplinary research program, referred to as the Southern California Behavioral Response Studies (SOCAL-BRS), has been conducted off southern California, USA since 2010, in order to understand marine mammal behavioral responses to military MFAS [10]. The study archival acoustic tags (e.g., DTAGs which are digital tags that attached to target animal by suction cups to track its movement and position, as well as to record sound [16]) to conduct controlled CEEs from animals exposed to simulated Navy MFAS pings [10, 17]. The simulated MFAS source used in the SOCAL-BRS was composed of a triad of upsweep and constant frequency tones projected from a 10-element vertical line array transducer. The transmitted ping had an initial 0.5 s linear frequency-modulated upsweep from 3.5–3.6 kHz, followed by a 0.5 s constant frequency tone at 3.75 kHz, then a 0.1 s silent period, and finally a 0.5 s constant frequency tone at 4.05 kHz. The total duration of the MFAS ping was 1.6 s, with a repetition rate of every 25 s from the onset of one ping to the onset of the next. Sound transmission was initiated at a broadband source level of 160 dB (RMS) re 1 μPa @ 1 m and ramp up at a 3 dB per ping to a maximum source level of 210 dB re 1 μPa @ 1 m.

During the SOCAL-BRS experiments in 2013 and 2014 seasons, passive acoustic recordings were made from drifting acoustic spar buoys deployed in the vicinity of the study sites. The drifting acoustic buoys were equipped with a HTI-96 hydrophone (nominal sensitivity of −180 dB re 1 V/μPa, with precise calibrated sensitivity used for each unique hydrophone). The hydrophone is attached to a pre-amplifier with a 20 dB gain, thus making the recording unit with a flat nominal sensitivity of −160 dB re 1 V/μPa (±3 dB) between 16 and 30000 Hz. The hydrophone was lowered to a depth of either 30 or 100 m below the surface, depending on the cable lengths of the drifting buoys being deployed. Acoustic data were recorded on high-density SD cards using an SM2M marine recorder (Wildlife Acoustics, Inc., Maynard, MA) housed in the instrument case of the drifting buoy. The sampling rate was set at either 50 kHz (for most of the 2013 season) or 80 kHz (for some 2013 and all 2014 seasons) on the SM2M recorder. To reduce noise generated from wave actions and cable strumming, a 3/16"-diameter bungee cord was use to link the buoy and the sensor, thus relieving the strain on the cable.

Deployments of the acoustic buoys were opportunistic within the SOCAL-BRS experiment, during periods when a DTAG was attached to the target animal and just prior to simulated MFAS CEEs or silent control sequences (see Southalll et al. [10] for a detailed description of SOCAL-BRS experiment design). The drifting buoys were either deployed from the source vessel R/V *Truth*, or from a dedicated pas-

Table 1. List of SOCAL-BRS sessions during which drifting acoustic buoy recorders were successfully deployed to collect sound field data. "Playback time" is the Pacific Daylight Saving Time, "Deploy vessel" is the vessel from which the drifting acoustic buoy recorder was deployed, "Dist." is the distance between the drift acoustic buoy and the source, and "S.R." is the sampling frequency

CEE No.	Date	Playback time	Deploy vessel	Dist., km	S.R., kHz
2013-13	12 September 2013	16:43–17:13	*Truth*	0.90	50
2013-14	14 September 2013	16:00–16:30	*Truth*	1.29	50
2013-20	23 September 2013	13:24–13:36	*Baylis*	2.48	80
2014-01	30 July 2014	15:54–16:24	*Truth*	1.98	80
2014-04	6 August 2014	12:01–12:31	*Truth*	1.92	80
2014-10	19 September 2014	11:02–11:32	*Baylis*	26	80

sive acoustic monitoring sailboat R/V *Baylis*. The buoy recorders were allowed to drift after the exposure sequence for at least an hour.

A total of six drifting acoustic buoy recorder deployments were successfully conducted to collect sound field data during CEE sequences (Table 1). During five of the deployments (CEEs 2013-14, 2013-20, 2014-01, 2014-04, and 2014-10), information of buoy locations during playbacks was also recorded on the embedded global positioning systems (GPS) in the instrument case of the buoys. Therefore, the distances between the buoys to the source vessel could be calculated. The distance of the acoustic buoy for CEE 2013-13 was obtained manually using range finding binoculars from R/V *Truth*.

Acoustic Data Analyses

To make consistent comparisons, the inter-ping sound field is defined as the acoustic field starting immediately after the ping and lasting for the following 23 s. The reason for excluding the final 2 s is to ensure the inter-ping sound field does not contain head wave of the subsequent ping that could result through bottom propagation, as shown in some studies done in the Arctic [18].

Acoustic data analyses were performed using custom MATLAB® (MathWorks, Natick, MA) algorithms written for this study. Continuous time history SPLs and spectrograms for each of the drifting acoustic buoy recording session were produced for visual inspection of the simulated MFAS playbacks and other pertinent acoustic information (e.g., passing vessels, cetacean vocalizations, etc.). The sound spectrograms were produced using Fast Fourier Transform (FFT) size of 2048 for 0.2 s (for recordings with a sampling rate of 50 kHz) segments or 0.5 s (for recordings with a sampling rate of 80 kHz) segments, with a Hamming window and no overlapping. The resulting spectrograms have a frequency resolution of 24.4 Hz and time resolution of 0.041 s for recordings with a sampling rate of 50 kHz, and a frequency resolution of 39.1 Hz and time resolution of 0.0256 s for recordings with a sampling rate of 80 kHz. None of the recordings during the simulated MFAS playback period contains detectable vessel noise. Therefore, the entire recordings during playback periods were used in the analyses.

For CEEs lasting the full 30 min duration, a total of 72 pings were transmitted. However, only pings with full SPL (i.e., 210 dB re 1 μPa @ 1 m) were used in the quantitative analyses described below, which exclude the initial 17 pings at lower SPLs below 210 dB. One playback (CEE 2013-20; September 23, 2013) was abruptly terminated after 12 min due to the detection of animals inside the safety zone, as required by the authorizing research permit. For this playback, only 11 pings occurred at the maximum SPL and were analyzed quantitatively. For recordings outside the simulated MFAS playback period, data with no detectable vessel noise were chosen for comparison to MFAS inter-ping sound field.

Frequency band specific SPLs of inter-ping intervals were computed using a numerical method, the incremental computation method (ICM). Specifically, simulated MFAS pings with full SPL were identified in each CEE sequence playback. The inter-ping intervals were then assigned as the 23-s duration after the 1.6-second simulated MFAS signal (Fig. 1). The inter-ping sound field levels were calculated on a series of 100 ms segments of RMS SPLs beginning immediately after the 1.6-s ping for the 23-s inter-ping interval (i.e., a total of 230 inter-ping SPLs segments were calculated after each simulated MFAS ping). The equation for calculating RMS SPLs is

$$SPL_{\mathrm{rms}} = 20\log\sqrt{\frac{1}{T}\frac{\int_0^T p^2(t)dt}{p_{\mathrm{ref}}^2}}, \qquad (1)$$

where SPL_{rms} is the RMS SPL, T is the time duration for the integral (100 ms), $p(t)$ is the instantaneous sound pressure, and p_{ref} is the referenced acoustic pressure of 1 μPa.

For recordings outside MFAS CEE sequences that do not contain detectable vessel noise through visual inspection of spectrograms, similar ICM was used to compute the natural background sound levels. For these periods, recordings 30-min after, or 30-min

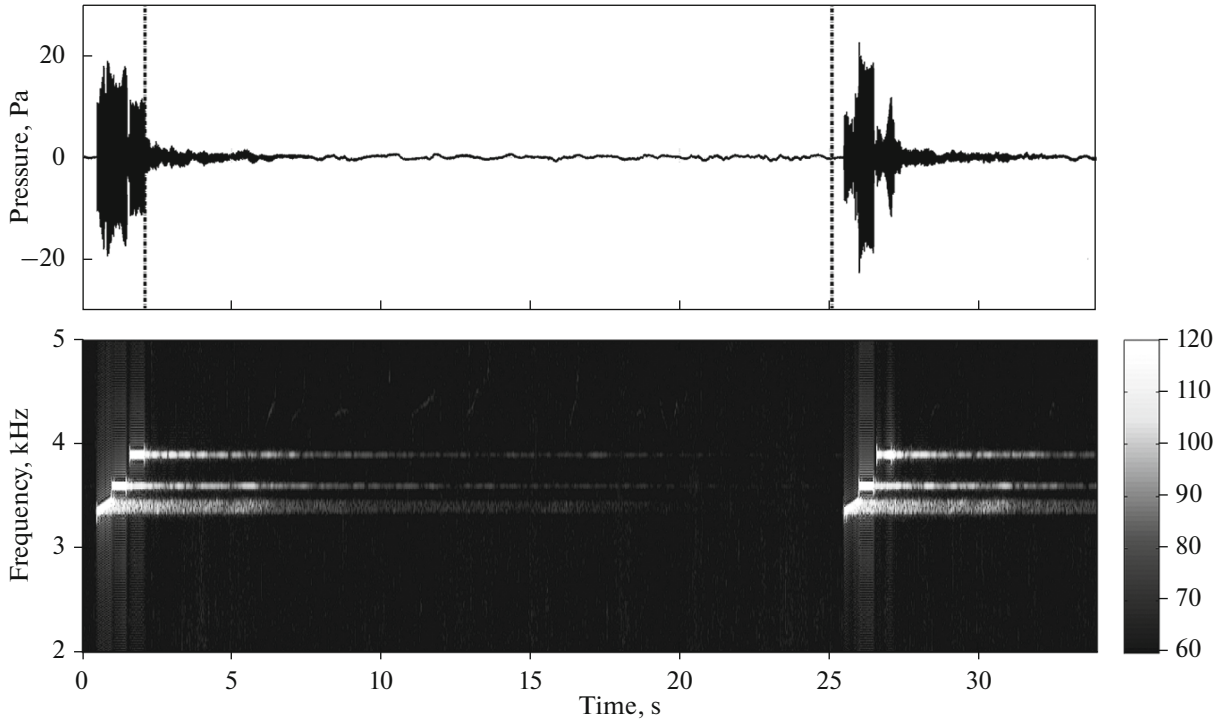

Fig. 1. Two simulated MFAS pings used in SOCAL-BRS, recorded at a distance of approximately 900 m from the source. The upper plat shows sound pressure time history and the lower one sound spectrogram. The interval between two vertical dotted lines shows the inter-ping interval between two pings. The inter-ping sound field is defined as the 23-s duration after the sonar ping.

before and after, simulated MFAS playbacks were computed for natural background noise levels. For CEEs nos. 2013-13 and 2013-14, there were not adequate recordings before the simulated MFAS playbacks, therefore, only natural background sound fields after the playbacks were computed. For the rest of the CEEs, both natural background sound field before and after playbacks were computed.

To evaluate the SPLs of natural background and inter-ping interval, median SPLs under different conditions (natural background vs. inter-ping) were calculated. Power spectral densities (PSDs) of median inter-ping sound field at the first 4, 4–8, 8–12, 12–16, and 16–20 s after the MFAS pings were plotted for five of the playback sessions.

Due to the band-limited nature of the simulated MFAS pings, spectral analysis was conducted in three distinctive frequency bands: low-frequency (<3 kHz), MFA-frequency (3–4.5 kHz), and high-frequency (>4.5 kHz) bands. Median levels of inter-ping sound levels for broadband, low-frequency, MFA-frequency, and high-frequency at different duration after the MFAS signals: 2, 4, 8, 12, 16, and 20 s, are compared with those of natural background sound levels for each playback session. A descriptive statistical analysis of inter-ping and natural background sound fields from the five SOCAL-13 and SOCAL-14 CEE sessions was conducted to show the mean, median, standard deviation, variance, and maximum and minimum values for each of the three frequency bands. In addition, kurtosis and skewness of the data sets were also computed to measure the outlier-prone of the distribution (kurtosis) and the asymmetry of the data around the mean (skewness). The equation for computing the kurtosis is

$$k = \frac{\frac{1}{n}\sum_{i=1}^{n}(x_i - \bar{x})^4}{\delta^4}, \quad (2)$$

and the equation for computing the skewness is

$$s = \frac{\frac{1}{n}\sum_{i=1}^{n}(x_i - \bar{x})^3}{\delta^3}, \quad (3)$$

where k is kurtosis, s is skewness, $\bar{x}$ is the mean of x, and δ is the standard deviation of x.

Additionally, the cumulative distributions of the results in three different frequency bands are assessed and compared with that of the natural background sound levels by employing the two-sample Kolmogorov–Smirnov tests [19].

Finally, inter-ping sound field decay curves were plotted to examine the behavior of reverberation decays of the sonar ping in the MFA-frequency band. The rates of decay were compared among recordings

collected from the drifting acoustic buoys at various known distances from the sites of playback.

RESULTS

A time–pressure plot and spectrogram of two MFAS pings recorded at a distance of approximately 900 m from the source are provided in Fig. 1. It can be noted that even at such a long distance, the peak pressure of the ping approaches 20 Pa, which is equivalent to 146 dB re 1 μPa. Time history plot of SPLs during CEE sessions shows clear MFAS pings, as shown in Fig. 2 for one of the CEE sessions (CEE 2013-13). Quantitative analyses of the simulated MFAS inter-ping sound field were performed on all playback recording sessions except CEE 2014-10 (September 19, 2014), because of the relatively greater distance (>26 km) of the drifting acoustic buoy from the source during this particular playback. Inter-ping intervals could not be determined from recordings obtained from that session due to the lack of distinctive onset of sonar pings.

Overall Comparison between Inter-ping Sound Field and Natural Background Levels

Averaged PSDs of the inter-ping sound field of 100 ms segments are plotted for the periods of 0–4, 8–12, and 16–20 s after the sonar ping (Fig. 3). These results indicate that the reverberant field of the sonar playback is highly band limited. Within the MFA-frequency band (3–4.5 kHz), strong inter-ping reverberant sound levels are obvious for at least the first 12 s after the ping, reaching approximately over 35 dB above natural background levels. The reverberant levels in the MFA-frequency band can be seen remain 10 dB above natural background even after 20 s after the sonar ping. In addition, it is observed that the acoustic energy output from even the first harmonic is much lower than the fundamental. The higher high-frequency energy of natural background in September 12, 2013, playback CEE 2013-13 (Fig. 3 top left) was from dolphin whistles prior to the MFAS playback. Comparison of median SPLs between natural background and inter-ping simulated MFAS playback for each of the five sessions are provided in Fig. 4. The comparisons were made for the three frequency bands for different duration being considered. The results also showed that even taking into consideration the full duration of the 23-s inter-ping interval, there is noticeable elevation of the inter-ping SPLs within the MFA-frequency band across the entire interval. However, outside the MFA-frequency band, there is almost no difference.

Descriptive Statistical Analyses

Results of a descriptive statistical analysis of inter-ping and natural background sound fields from the five SOCAL-13 and SOCAL-14 CEE sessions that show the mean, median, standard deviation, variance, maximum and minimum values, kurtosis and skewness for each of the three frequency bands are provided in Table 2.

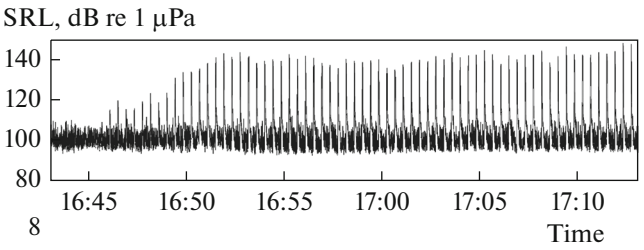

Fig. 2. SPL plot of simulated MFAS playback (CEE 2013-13) on September 12, 2013.

In the low-frequency band (<3 kHz), the maximum value of the inter-ping sound field occurs 12 s after the MFAS ping. Both mean and median SPLs of inter-ping sound field are slightly lower than the natural background in this frequency band. These results indicate that sound field in this frequency band is not influenced by the reverberant field of the MFAS ping. The kurtosis and skewness of the inter-ping sound field at various duration in the low-frequency band are quite similar, between 4.1 and 4.3 for kurtosis and between 0.70 and 0.88 for skewness. This suggests that the distributions of the inter-ping sound fields at the lower frequency band are very similar, with slight skewness towards right. In addition, the relatively low standard deviation and variance suggest that the SPL values from this frequency band are not very dispersed.

In the MFA-frequency band (3–4.5 kHz), the mean and median SPL values of inter-ping sound field exceed those natural background levels by at least 9 and 5 dB, respectively (Table 2). Especially during the first 16 s (or approximately 75% of the inter-ping interval), the differences are more than 13 dB for mean and 10 dB for median SPLs. The maximum SPL of 130 dB re 1 μPa occurred within the first 2 s after the MFAS ping. Among various duration of the inter-ping sound field in the MFA-frequency band, the standard deviation and variance show much wider range with increasing in duration, suggesting greater dispersion of the SPLs with the decaying process. For example, the standard deviation begins at 4.70 at the end of the 2nd s to almost 12 by the end of 12 s. The variances increased from about 22 at the end of the 2nd s to over 140 at the end of 16 s. This suggests that the inter-ping SPLs have much greater variation in the inter-ping interval, and is likely due to the reverberant decaying process. Kurtosis and skewness in the MFA-frequency band also varied over the full duration, from about 11 at the end of first 2 s down to 1.7 at the end of 12 s then back up to about 2.5 by the end of 23 s for kurtosis. Skewness of the MFA-frequency band inter-ping sound field

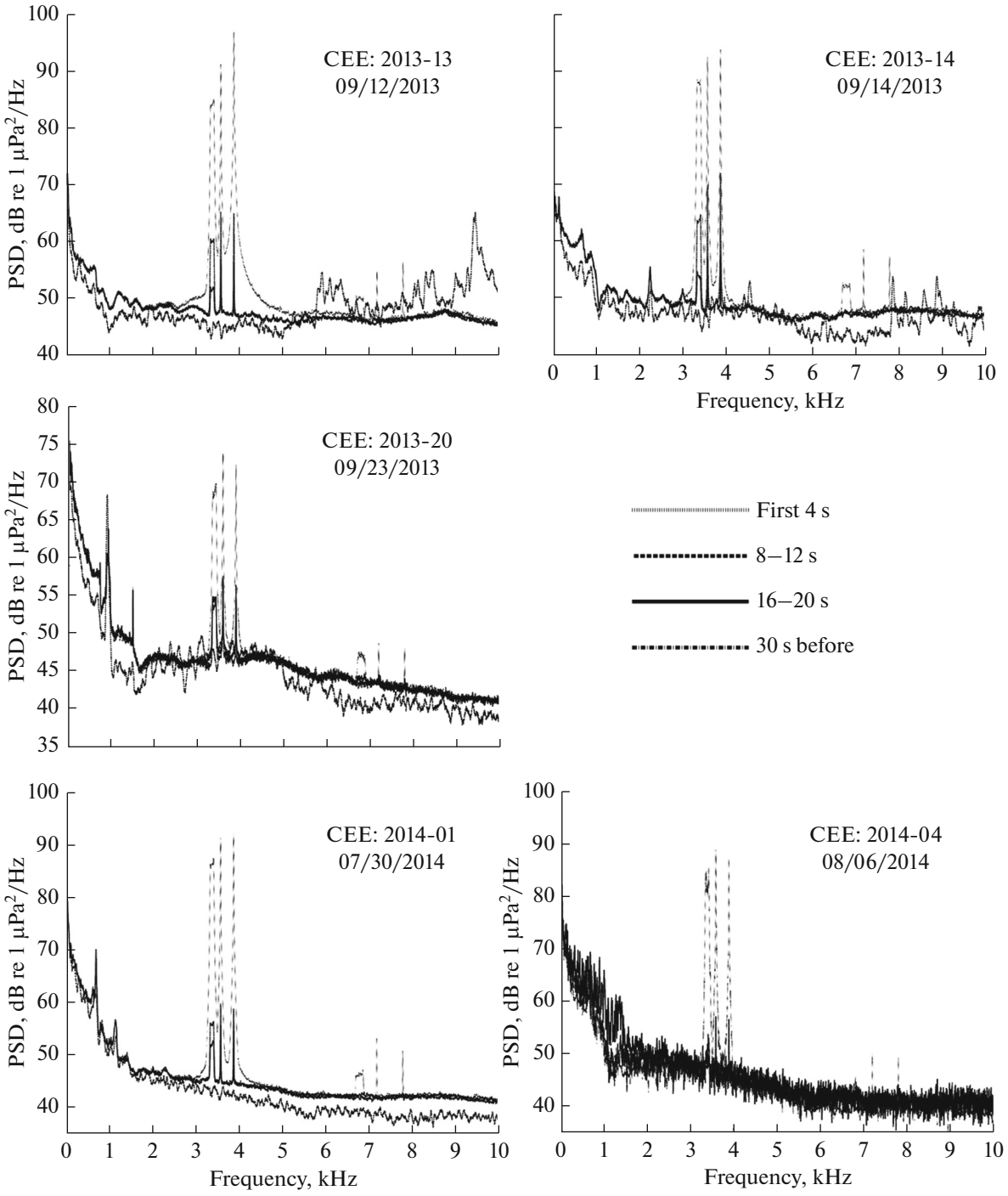

Fig. 3. Mean PSD of simulated MFAS inter-ping sound field for the periods of 0–4, 8–12, and 16–20 s after the sonar ping, as well as 30 min before the onset of ping for comparison.

shifted from −1.28 at the end of 2 s after MFAS ping to 0.96 by the end of the inter-ping interval. This is also illustrated by a gradual shift of the shape of the SPL distribution from left-skewed to right-skewed with the progression through the inter-ping interval (Fig. 5).

For the high-frequency band (>4.5 kHz), the inter-ping SPLs are of similar values to that of natural background, at least for the later portion of the sound field at 8 s after the MFAS ping. The SPLs of the first 4 s inter-ping sound field are about 2 dB above the natural background level and show a slight decay pattern. The small values of standard deviation and variance indicate that the SPLs in this frequency band have even less variation than those from the low-frequency band.

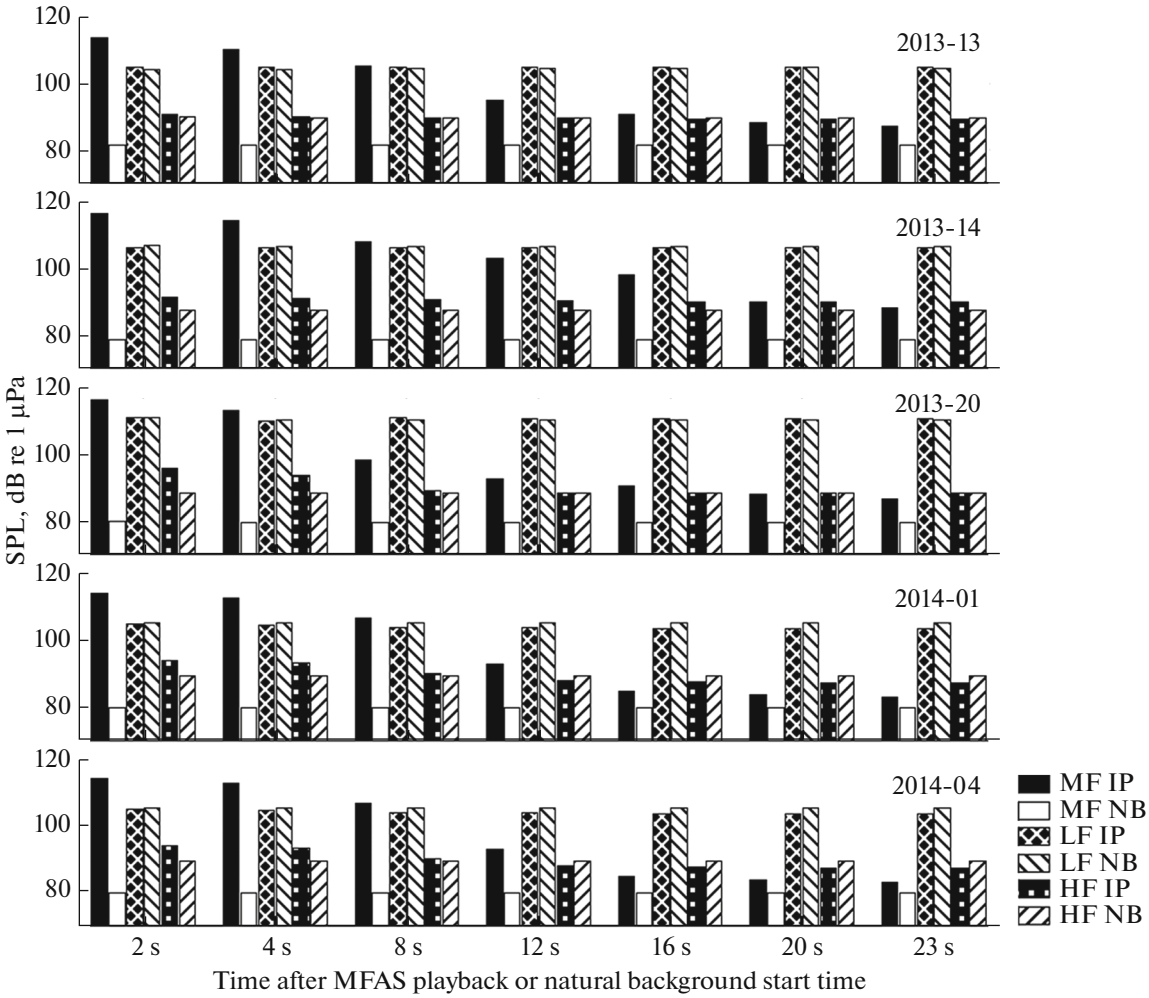

Fig. 4. Median ICM SPLs comparison between MFAS inter-ping (IP) and natural background (NB) sound fields for three different frequency bands at different duration after the MFAS ping or the start of natural background measurements. LF: low-frequency band (<3 kHz), MF: MFA-frequency band (3–4.5 kHz), HF: high-frequency band (>4.5 kHz). For CEEs 2013-13 and 2013-14, the natural background measurements started from 30-min acoustic recordings after simulated MFAS playback. For CEEs 2013-20, 2014-01, and 2014-04, the natural background median levels are the averages starting from both 30-min acoustic recordings before and 30-min after simulated MFAS playback.

The kurtosis increases from about 4 to 8 from the first 4 s to the end of the inter-ping sound field, suggesting the ever converging SPL values. The skewness increases slightly from slightly over 1 to 2 from the first 2 s to the end of the inter-ping sound field, suggesting the ever shifting distribution shape skewed towards the right.

Median SPL Distributions and Cumulative Percentiles

The distributions and cumulative percentile of the median SPLs of inter-ping sound field for three different frequency bands (<3, 3–4.5, and >4.5 kHz) at different duration (4, 8, 12, 16, and 20 s) after the simulated MFAS ping and that of natural background for all five MFAS playback sessions are show in Fig. 5. This figure clearly reflects the statistical analysis presented in Table 2 above. Of particular interesting are the SPL distribution curves for the inter-ping sound field. These curves at different duration undergo rather abrupt shifts of mode between 8 and 16 s after the ping. For the first two duration (4 and 8 s after the sonar ping), the modes of the inter-ping SPLs are around 110 dB re 1 μPa, while after 16 s the mode of the SPLs drops to about 80 dB re 1 μPa. At 12 s after the sonar ping, it appears to have a bi-modal at 80 and 105 dB re 1 μPa (Fig. 5).

Kolmogorov–Smirnov Tests

Two-sample Kolmogorov–Smirnov tests of the cumulative distribution curves were performed to investigate the significance of the differences between inter-ping sound field and natural background levels,

Table 2. Descriptive statistics of inter-ping SPLs at different duration after the sonar ping and natural background sound field from the five SOCAL-13 and SOCAL-14 CEEs, showing mean, median (Med), standard deviation (Std), variance (Var), maximum (Max) and minimum (Min) SPLs, kurtosis (Kurt), and skewness (Skew). LF: low-frequency band (<3 kHz), MF: MFA-frequency band (3–4.5 kHz), HF: high-frequency band (>4.5 kHz), NB: natural background, IP: inter-ping. SPLs are expressed in dB re 1 μPa

	Mean	Med	Std	Var	Max	Min	Kurt	Skew
LF NB	106.58	106.15	4.85	23.52	131.45	91.60	4.33	0.70
LF IP 23s	104.95	104.01	4.76	22.70	129.56	91.84	4.12	0.83
LF IP 20s	104.96	104.03	4.76	22.67	129.56	91.84	4.18	0.84
LF IP 16s	105.00	104.10	4.71	22.14	129.56	91.84	4.11	0.81
LF IP 12s	105.08	104.20	4.71	22.18	129.56	91.84	4.16	0.81
LF IP 8s	105.23	104.37	4.71	22.21	129.36	91.84	4.28	0.84
LF IP 4s	105.40	104.64	4.38	19.17	125.32	93.39	4.10	0.79
LF IP 2s	105.60	104.85	4.25	18.05	124.46	95.14	4.11	0.88
MF NB	81.16	80.72	3.39	11.51	100.31	74.06	4.87	1.02
MF IP 23s	90.67	85.35	11.76	138.28	130.40	75.33	2.53	0.96
MF IP 20s	92.12	86.78	11.91	141.90	130.40	75.77	2.20	0.78
MF IP 16s	94.71	90.02	11.96	142.94	130.40	77.78	1.84	0.49
MF IP 12s	98.29	98.88	11.69	136.76	130.40	77.83	1.70	0.06
MF IP 8s	104.47	106.05	8.98	80.62	130.40	79.40	2.55	–0.45
MF IP 4s	111.17	110.79	4.90	24.03	130.40	79.40	7.61	–0.67
MF IP 2s	113.46	114.08	4.70	22.13	130.40	79.40	11.20	–1.28
HF NB	89.82	88.98	2.56	6.58	108.58	86.61	5.76	1.62
HF IP 23s	89.22	88.47	2.63	6.89	108.28	86.40	8.02	1.99
HF IP 20s	89.31	88.56	2.67	7.13	108.28	86.40	7.65	1.93
HF IP 16s	89.49	88.73	2.74	7.52	108.28	86.40	7.27	1.85
HF IP 12s	89.79	90.00	2.84	8.08	108.28	86.40	6.68	1.73
HF IP 8s	90.34	89.51	2.90	8.44	108.28	86.58	5.93	1.57
HF IP 4s	91.53	90.68	2.99	8.94	108.28	87.06	4.66	1.29
HF IP 2s	92.09	91.26	3.11	9.69	108.28	87.30	4.32	1.16

Table 3. Two-sample Kolmogorov–Smirnov tests of the cumulative distribution curves between inter-ping sound filed and natural background levels, and among inter-ping sound field for different duration after the sonar ping. LF: low-frequency band (<3 kHz), MF: MFA-frequency band (3–4.5 kHz), HF: high-frequency band (>4.5 kHz), NB: natural background, IP: inter-ping

Kolmogorov–Smirnov test pairs	*P*-value
LF IP 23s vs. LF NB	$P = 1$
MF IP 23s vs. MF NB	$P < 0.01$
HF IP 23s vs. HF NB	$P = 1$
MF IP 23s vs. MF IP 20s	$P < 0.01$
MF IP 23s vs. MF IP 16s	$P < 0.01$
MF IP 23s vs. MF IP 12s	$P < 0.01$
MF IP 23s vs. MF IP 8s	$P < 0.01$
MF IP 23s vs. MF IP 4s	$P < 0.01$
MF IP 23s vs. MF IP 2s	$P < 0.01$

and among inter-ping sound field at different duration. The results show that there are no significant differences between inter-ping sound field and natural ambient SPLs in both the low- (<3 kHz) and high-frequency (>4.5 kHz) bands. However, significant differences in the cumulative distribution curves are found between MFA-frequency band (3–4.5 kHz) inter-ping sound field and natural background SPLs, and among inter-ping sound field at different duration after the sonar ping (Table 3).

Inter-Ping Sound Field Decay

Inter-ping sound field decay curves (Fig. 6) show that the duration of elevated sound levels within the inter-ping interval depends on the distance from the source. At a distance of 900–1300 m (CEEs 2013-13 and 2013-14; September 12 and 14, 2013), the inter-ping sound field remains 5 dB above natural background for over 15 s after the ping, or 65% of the entire inter-ping interval. At a distance of approximately

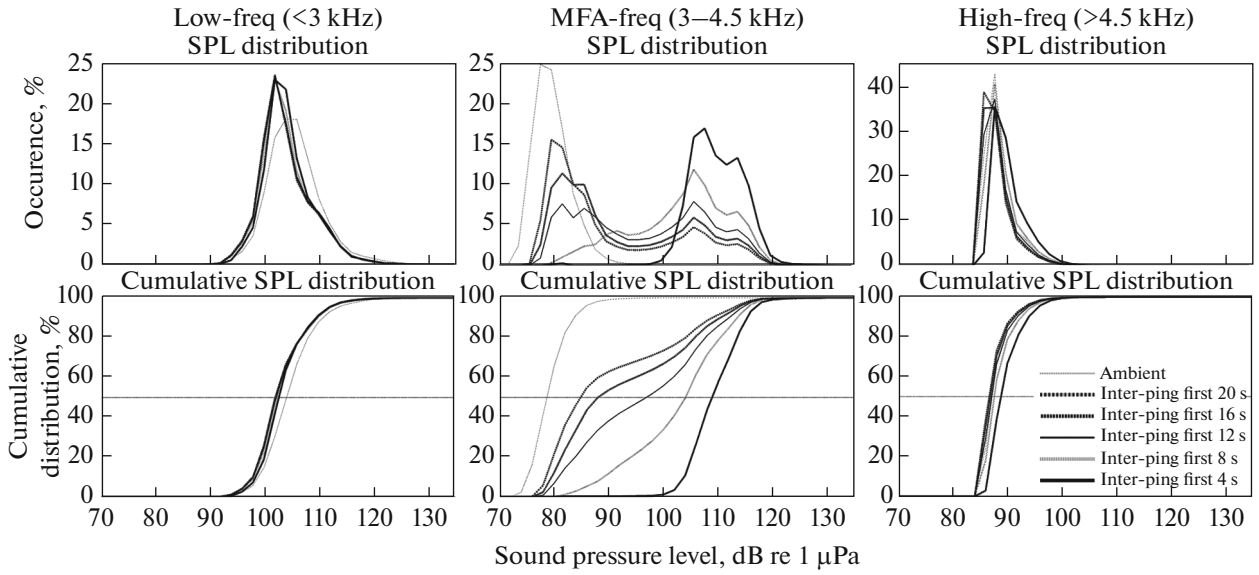

Fig. 5. The distribution of the median SPLs of inter-ping sound field for three different frequency bands (<3, 3–4.5, and >4.5 kHz) at different duration (4, 8, 12, 16, and 20 s) after the simulated MFAS ping and natural background (upper) and the cumulative percentile of these values (lower) from all five collected recordings of SOCAL-13 and SOCAL-14 CEEs.

2000 m (CEEs 2014-01 and 2014-04; July 30 and August 6, 2014), the inter-ping sound field stays 5 dB above for only about 7 s after the ping, or 30% of the inter-ping interval. CEE 2013-20 (September 23, 2013) was terminated after 11 full-power ping transmissions, and was recorded by the acoustic buoy at a distance of about 2500 m. This session has a relatively high natural background level of approximately 83 dB re 1 μPa in the MFA-frequency band. Nevertheless, it shows that the inter-ping sound field remains over 5 dB above the natural background level for at least 12 s after the ping. The initial SPLs of the inter-ping sound field shows great variation among the data collected. The initial inter-ping SPLs range between 107 and 119 dB re 1 μPa for sources at about 2000–2500 m, or about 27–36 dB above the natural background. At source distances of 900 and 1300 m, the initial inter-ping SPLs are at 125 and 117 dB re 1 μPa, or about 44 and 43 dB above the natural background at the time, respectively.

The results of this study show an overall increase of 20–40 dB in the first 5 s after the ping within the MFA-frequency band. Adding an additional 1.6 s of the simulated MFAS duration, makes a total of 6.6 s of elevated noise levels above 20–40 dB above natural background levels for every 25 s (or 36% of the entire MFAS playback duration).

DISCUSSION

We utilized drifting acoustic recording buoys to more fully describe the background noise level and reverberant sound field during noise exposure in a marine mammal biological and behavioral response study using CEEs off southern California. These results augment the SOCAL-BRS analyses [10] by providing several more detailed quantitative analyses of acoustic exposure data not possible to obtain from archival acoustic tags attached to highly mobile, free-ranging animals.

Although a casual visual inspection received acoustic exposure during MFAS playbacks does not reveal a strong difference of inter-ping sound field levels from those of natural background (Fig. 2), detailed quantitative analyses show clear elevation of inter-ping noise levels within the MFA-frequency band (3–4.5 kHz) for all five CEE sessions investigated (Fig. 4). In addition, sonar pings were distinguishable at a distance at least 2.48 km away from the source. Two-sample Kolmogorov–Smirnov tests show a significant difference between the inter-ping sound field and natural background levels within the MFA-frequency band, but no difference outside the MFA-frequency band (Table 3). All these results suggest that elevated noise levels between brief sonar pings should not be overlooked when addressing potential noise effects on marine life, particularly to the extent that they may overlap with important biological signals and/or reveal important contextual aspects of exposure (e.g., information about relative proximity of the sound source) that may influence the probability of behavioral response.

Our results show that the sound field is not affected by the sonar ping in the frequencies below the MFA-frequency band. In the high-frequency band, however, there is 2 dB increase in the inter-ping interval immediately after the sonar ping (Table 2). This increase is evidently a result of harmonics of the MFAS pings, as

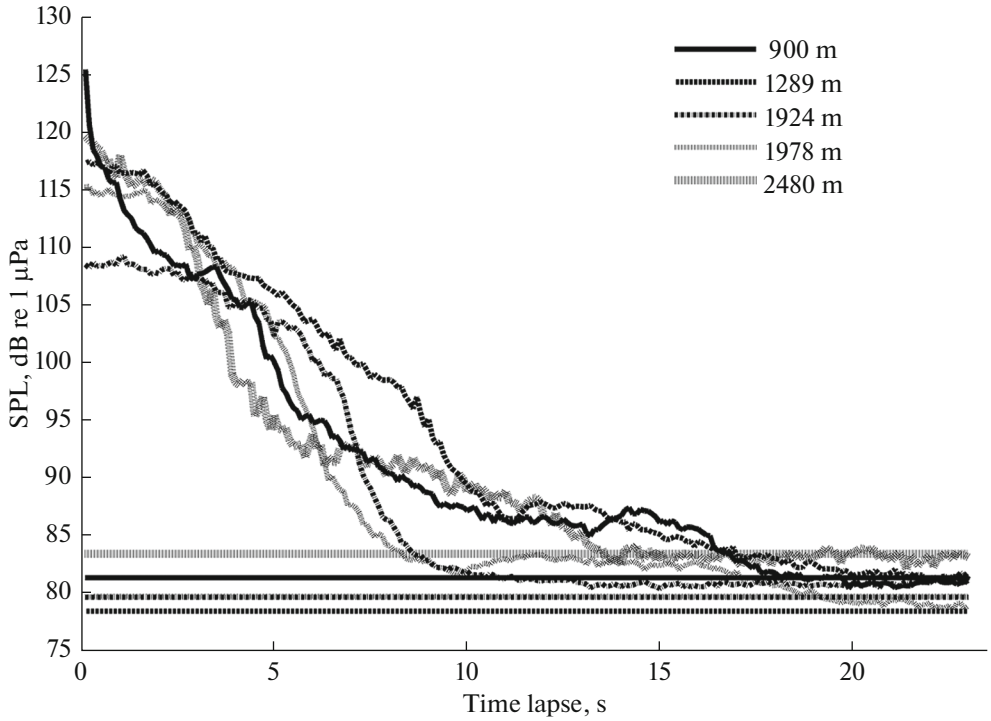

Fig. 6. Inter-ping sound field decays and their natural background levels in the MFA-frequency band (3–4.5 kHz) for sonar playbacks at different source–buoy distances.

shown in the PSD plots in Fig. 3. Nevertheless, this slight inter-ping increase from harmonics had a much faster decay to the baseline levels when compared to the inter-ping sound field in the MFA-frequency band. The presence of harmonic components and their respective strength and prevalence relative to the primary energy of the signals may provide relevant contextual information about source proximity that could affect how animals respond to such exposures [9].

Conventional thinking is that narrowband noise sources are likely to have little effect on animals' acoustic communication outside the source band. Thus, for the MFAS, due to its tonal feature and short duration, there would logically be negligible acoustic masking. However, studies in human psychoacoustics demonstrate that tonal noise can effectively raise hearing threshold beyond the frequency band where the masking tone is [20, 21]. Studies also show that for acoustic masking outside the masker frequency spectrum, the degree of masking is more pronounced at frequencies above the masking tone than below it, which is known as the upward spread of masking [22]. Research on pure tone masking on a bottlenose dolphin (*Tursiops truncatus*) demonstrated elevated signal detection threshold outside the masking band, though the degrees of masking are approximately the same on both sides of the masking frequency [23]. While the potential upward spread of masking from the relatively lower overall levels present in reverberant acoustic field may be relatively limited, clearly these aspects of potential masking within and somewhat above the exposure frequency band should be considered in subsequent studies.

The decay rates of the sonar ping determine the duration of the inter-ping SPLs staying above natural background levels. The reverberation decay of sound ranging devices in the ocean has been previously studied in the advancement of sonar development (e.g., Eckart [24] and Chapman and Marshall [25]). To maximize detection range, typical operational active sonars are also designed to emit signals with very high source levels. However, the increase of source level would also elevate the reverberation level within the frequency band of interest [26]. Thus, to achieve the optimum performance, reverberant levels and other factors must be considered. The maximum source level for the simulated MFAS used in SOCAL-BRS is 210 dB re 1 μPa [10], which is 25 dB lower than the unclassified source levels for AN/SQS-53 series of MFASs used by U.S. Navy and its allies [27]. Therefore, it is expected the inter-ping sound field levels resulting from these actual military sonars would be substantially higher, and the duration of the elevated inter-ping SPLs would be longer than the results obtained from this study, provided that other conditions such as the distance and environment are the same. Unfortunately, due to the limited data sets and many unknown environmental parameters (such as water depth, sound velocity profile, weather conditions) in this preliminary study, precise decay rates

cannot be established (Fig. 6). In addition, since this is an opportunistic study based on SOCAL-BRS, drifting acoustic buoys were deployed whenever chances were available. Thus, the distances between the acoustic buoy and the source were not taken into consideration during the deployment. Subsequent effort within the SOCAL-BRS effort is including CEEs with real 53C systems and will provide clearly needed quantitative measurements of reverberant decay of inter-ping sound field. Finally, this study also calls for future research on monitoring impacts to marine life from other transient anthropogenic noise sources such as seismic airgun pulses [28, 29] to include reverberant sound field analyses.

CONCLUSIONS

This study includes novel measurements to more full describe and quantify ambient noise and the reverberant sound field generated from a tonal transient anthropogenic noise source within marine mammal CEEs. The objective was to better understand aspects of the exposure context related to exposure reverberation that may have particular bearing on behavioral response probability (e.g., information animals may obtain about source proximity) and the potential acoustic masking of marine mammal communication. The results show significantly elevated SPLs in the inter-ping interval of the MFA-frequency band when compared to natural background levels before and after MFAS playbacks. No difference is observed between inter-ping SPLs and natural background levels in the low- and high-frequency bands. In addition, the duration of elevated inter-ping sound field depends on and thus may convey information about the MFAS source distance from subjects. At ranges of 900–1300 m from the source, the inter-ping sound field is observed to remain 5 dB above natural background levels for approximately 15 s, or 65%, of the entire inter-ping interval. However, at a range of 2000 m, the 5 dB elevation of the inter-ping SPLs only lasted for about 7 s, or 30% of the inter-ping interval.

The prolonged elevation of sound field beyond the brief sonar ping at greater ranges underscores the need for further studies on potential context-based behavioral responses and potential masking effects associated with source reverberation. While direct-path exposure to much higher-level MFAS pings are certainly important, animals may react differently based on sound characteristics of the reverberant field in ways that should be described and considered [9]. Future behavioral response studies should thus incorporate measurements of the overall sound field and natural background sound levels in the vicinity of the study area.

ACKNOWLEDGMENTS

The authors are grateful for some drifting acoustic buoy recordings provided by Dr. Jay Barlow of the U.S. National Marine Fisheries Service Southwest Fisheries Science Center. The authors thank for the crew of R/V *Truth* and R/V *Baylis* for assistance during the field work, as well as the assistance and support of all the SOCAL-BRS field teams, led by John Calambokidis. The socal-BRS was supported by the U.S. Navy's Living Marine Resources Program and the Office of Naval Research Marine Mammal Program. All research described here was conducted under and in compliance with the terms of U.S. National Marine Fisheries Service marine mammal research permit # 14534.

REFERENCES

1. A. Frantzis, Nature **392**, 29–30 (1998).
2. K. C. Balcomb, III and D. E. Claridge, Bahama J. Sci. **8**, 2–12 (2001).
3. M. Schrope, Whale deaths caused by US Navy's sonar. Nature **415**, 106–106 (2002).
4. T. J. Cox, A. J. Ragen, A. J. Read, E. W. Baird, K. Balcomb, J. Barlow, J. Caldwell, T. Cranford, L. Crum, A. d'Amico, G. d'Spain, A. Fernandez, J. Finneran, R. Gentry, W. Gerth, et al., J. Cetacean Res. Manag. **7**, 177–187 (2006).
5. R. Filadelfo, J. Mintz, E. Michlovich, A. D'Amico, P. L. Tyack, and D. R. Ketten, Aquatic Mamm. **35**, 435–444 (2009).
6. P. D. Jepson, M. Arbelo, R. Deaville, I. A. P. Patterson, P. Castro, J. R. Baker, E. Degollada, H. M. Ross, P. Herráez, A. M. Pocknell, F. Rodríguez, F. E. Howie, A. Espinosa, R. J. Reid, et al., Nature **425**, 575–576 (2003).
7. P. D. Jepson, R. Deaville, I. A. P. Patterson, A. M. Pocknell, H. M. Ross, J. R. Baker, F. E. Howie, R. J. Reid, A. Colloff, and A. A. Cunningham, Veterinary Pathol. **42**, 291–305 (2005).
8. S. K. Hooker, A. Fahlman, M. J. Moore, N. Aguilar de Soto, Y. Bernaldo de Quirós, A. O. Brubakk, D. P. Costa, A. M. Costidis, S. Dennison, K. J. Falke, A. Fernandez, M. Ferrigno, J. R. Fitz-Clarke, M. M. Garner, D. S. House, et al., Proc. Royal Soc., London, Biolog. Sci. **279**, 1041–1050 (2012).
9. W. T. Ellison, B. L. Southall, C. W. Clark and A. S. Frankel, Conser. Biol. **26**, 21–28 (2012).
10. B. L. Southall, D. Moretti, B. Abraham, J. Calambokidis, S. L. DeRuiter, and P. L. Tyack, Mar. Technol. Soc. J. **46** (4), 48–59 (2012).
11. C. W. Clark, W. T. Ellison, B. L. Southall, L. Hatch, S. M. Van Parijs, A. Frankel, and D. Ponirakis, Mar. Ecol. Prog. Ser. **395**, 201–222 (2009).
12. M. Guerra, A. M. Thode, S. B. Blackwell, and A. M. Macrander, J. Acoust. Soc. Amer. **130**, 3046–3058 (2011).
13. S. Guan, J. Vignola, J. Judge, and D. Turo, J. Acoust. Soc. Amer. **138** (6), 3447–3457 (2015).
14. W. J. Richardson, C. R. Greene Jr., C. I. Malme, and D. H. Thomson, *Marine Mammals and Noise* (Aca-

demic Press, San Diego, CA, 1995). Sect. 8.5.2. pp. 229–233.

15. W. W. L. Au and M. C. Hastings, in *Principles of Marine Bioacoustics* (Springer Science + Business, New York, NY, 2008). Sect. 9.2.2.1.
16. M. P. Johnson and P. L. Tyack, IEEE J. Oceanic Engin. **28**, 3–12 (2003).
17. B. Southall, J. Calambokidis, J. Barlow, D. Moretti, A. Friedlaender, A. Stimpert, A. Douglas, K. Southall, P. Arranz, S. DeRuiter, E. Hazen, J. Goldbogen, E. Falcone, and G. Schorr, in *Biological and Behavioral Response Studies of Marine Mammals in Southern California,* 2013 ("SOCAL-13"). (Aptos, CA, 2014).
18. HDR Alaska, Inc., in *NMFS 90-day report for marine mammal monitoring and mitigation during BPXA Simpson Lagoon OBC seismic survey*, Beaufort Sea, Alaska, July to September 2012. (Anchorage, AK, 2013).
19. J. H. Drew, A. G. Glen, and L. M. Leemis, Computational Statistics & Data Anal. **34**, 1–15 (2000).
20. J. P. Egan and H. W. Hake, J. Acoust. Soc. Am. **22** (5), 622–630 (1950).
21. R. L. Wegel and C. E. Lane, Phys. Rev. **23**, 266–285 (1924).
22. B. C. J. Moore, Psychoacoustics, in *Springer Handbook of Acoustics*, Ed. by T. Rossing (Springer, New York, 2007). Sect. 13.2.4. pp. 464–465.
23. C. S. Johnson, J. Acoust. Soc. Am. **49** (4B), 1317–1318 (1971).
24. C. Eckart, in *Principles of Underwater Sound* (National Research Council, Wakefield, MA, 1946). Sect. 5.4.3. pp. 104–109.
25. R. P. Chapman and J. R. Marshall, J. Acoust. Soc. Am. **40** (2), 405-411 (1966).
26. R. J. Urick, in *Principles of Underwater Sound* (McGraw-Hill, New York, 1983). Sect. 12.8. pp. 395–396.
27. J. A. Hildebrand, "Impacts of anthropogenic sound," in *Marine Mammal Research: Conservation Beyond Crisis*, Ed. by J. E. Reynolds, III, W. F. Perrin, R. R. Reeves, S. Montgomery, and T. J. Ragen (Johns Hopkins University Press, Baltimore, 2005), Chapt. 7. pp. 101–124.
28. A. N. Rutenko, A. V. Gavrilevskii, D. G. Kovzel', R. A. Korotchenko, V. F. Putov, and A. A. Solov'ev, Acoust. Phys. **58**, 210–219 (2012).
29. A. N. Rutenko, D. I. Borovoi, V. A. Gritsenko, P. S. Petrov, V. G. Ushchipovskii, and M. Boekholt, Acoust. Phys. **58**, 326–338 (2012).